

Growth and magnetic properties of MnO_2 nanowire microspheres

J.B. Yang, X.D. Zhou, W.J. James

Graduate Center for Materials Research and Departments of Physics and Chemistry, University
of Missouri-Rolla, Rolla, MO 65409

S.K. Malik

Tata Institute of Fundamental Research, Colaba, Mumbai 400-005, India

C.S. Wang

School of Physics, Peking University, Beijing 100871, P.R. China

Abstract

We report the synthesis of MnO_2 microspheres using hydrothermal and conventional chemical reaction methods. The microspheres of MnO_2 consist of nanowires having a diameter of 20-50 nm and a length of 2-8 μm . The value of the oxygen vacancy estimated from the x-ray photoelectron spectrum (XPS) is 0.3. The magnetization versus temperature curve indicates a magnetic transition at about 13 K. It is found that a parasitic ferromagnetic component is imposed on the antiferromagnetic structure of MnO_2 , which might result from distortion of the lattice structure due to oxygen vacancies. The magnetic transition temperature T_N is about 10 K lower than that of the bulk MnO_2 single crystal.

PACS numbers: 61.46 + w, 75.75 + a, 75.50 -y 81.07 -b

The possibility of controlling the structure and the chemical composition of materials at the nanoscale level is of great interest for both basic science and technological applications. In particular, one dimensional (1-D) nanometric structures of oxides have attracted intensive attention [1-4]. For example MnO_2 has distinctive properties which have enabled its use as catalysts, ion-sieves, and electrode materials [5-7]. Both α - and β - MnO_2 are potential candidates for cathodes and catalysts in Li/MnO_2 batteries [5]. They can be converted into $\text{Li}_{1-x}\text{Mn}_2\text{O}_4$ cathode by electrochemical Li^+ intercalation, in which Li^+ was inserted or extracted during the charging or discharge process. MnO_2 nanowires are of great interest due to that their morphology simultaneously minimize the distance over which Li^+ must diffuse during the discharge and charging processes [8]. This may provide the opportunity to determine the theoretical operating limits of a Lithium battery as the 1-D nanowire is the smallest structure for the efficient electron transport. MnO_2 nanowires or nanostructure materials also contain much highly surface area which may become more ideal host materials for the insertion and extraction of lithium ions and chemical reactions. Therefore, well-defined 1-D nanostructures appear as a much better candidate for studies on the space-confined transport phenomena as well as applications. Considerable effort has been made to prepare bulky or nanocrystalline MnO_2 with different structures [9-12]. Recently, single crystal MnO_2 nanowires have been synthesized using a hydrothermal method [13]. MnO_2 also possesses an interesting magnetic structure [14-17]. Up to now, very few investigations on the magnetic properties of nano-sized Mn-oxides have been reported. In this letter, we report the synthesis of microspheres of MnO_2 consisting of nanowires. The microspheres were prepared using both hydrothermal and room temperature chemical reaction methods. The structure, morphology, composition and magnetic properties of the Mn-oxide microspheres were studied using x-ray diffraction (XRD), scanning electron microscopy (SEM), transmission electron microscopy (TEM), magnetic measurements and x-ray photoelectron spectroscopy (XPS).

The materials synthesized here were prepared by oxidation of hydrated manganese sulfate $\text{MnSO}_4 \cdot \text{H}_2\text{O}$ with an equal amount of ammonium persulfate $(\text{NH}_4)_2\text{S}_2\text{O}_8$ [13].

$\text{MnSO}_4 \cdot \text{H}_2\text{O}$ (0.08 mol) and $(\text{NH}_4)_2\text{S}_2\text{O}_8$ (0.08 mol) were dissolved in 150 ml distilled water at room temperature to form a clear solution. Half of the solution was transferred into a stainless steel autoclave, sealed and maintained at 120 °C for 12 h. Another half of the solution was kept at room temperature in air for 6 h. After the reaction, the resulting black solid from each solution was filtered and washed with distilled water and acetone several times, then dried at 60 °C for 24 h. X-ray diffraction (XRD) using Cu-K α radiation shows the material to be single phase, $\gamma\text{-MnO}_2$. The magnetization curves of the samples were measured using a SQUID magnetometer in a field of up to 6 T from 1.5 K to 300 K. The morphology was studied using SEM (JEOL-6340F) and TEM. X-ray photoelectron spectra were collected using a "KRATOS" model AXIS 165 XPS spectrometer with a Mg source and an Al monochromator.

Fig. 1 shows the x-ray diffraction patterns of the samples obtained by both methods. The diffraction peaks can be indexed to $\gamma\text{-MnO}_2$ with lattice parameters $a = 9.784 \text{ \AA}$ and $c = 2.863 \text{ \AA}$, space group $I4/m$. The XRD pattern of the room temperature treated sample (Fig. 1(b)) shows much broader, and less intensive peaks, due to its smaller grain size and the many crystal defects. There are some changes in the relative peak intensities in Fig. 1(b), suggesting a preferred orientation among the Mn-oxide grains. The mean size of the particles (Fig. 1(a)) is about 40 nm as determined by the Scherrer formula using the width of the [211] peak from Fig. 1(a), and was further confirmed by SEM and TEM imaging (Fig. 2).

Fig. 2 shows the SEM ((a)-(d)) and TEM (e) images of the samples prepared by the two methods. Figs. 2(a) and (b) show a sea urchin-like sphere with a diameter of 4-8 μm for the sample prepared by the hydrothermal method. These microspheres consist of bundles of small wires with a diameter of 20-50 nm (see TEM image (e)). Figures 2(c) and (d) show the typical morphology of the MnO_2 obtained by the reaction carried out at room temperature. The diameter of these microspheres varies from 1 to 4 μm . The microspheres are also made up of smaller needle-like wires, however, they are not so sharply defined as compared to the samples made by the hydrothermal method. The hydrothermal treatment

increases the diameter of the microspheres and the length of the nanowires. It is found that the concentration of the solution is very important in forming the microspheres. The microspheres can be synthesized when the Mn^{2+} concentration is higher than 0.3 mol/L. It suggests that, at high Mn^{2+} concentrations, the formation of microspheres by aggregation of the nanowires is favored by a decrease in the total surface energy of the system.

A typical room temperature x-ray photoelectron spectrum of the Mn_2 prepared by the hydrothermal method is plotted in Fig. 3. The peaks of Mn (3s, 3p, 2p, 2s) and O (1s, 2s) are observed. Auger peaks from Mn and O are also observed as O KLL and Mn LMM lines. The binding energies of the Mn 2p_{3/2} and 2p_{1/2} states are 641.5 and 653.6 eV, respectively, which are lower than those of the standard MnO_2 (642.1 and 653.8 eV) [18]. The decrease in binding energy is likely due to the oxygen vacancies formed in these materials which would decrease the Mn-O bond strength. The estimated relative ratio of Mn to O is 37:63 corresponding to a composition of about $MnO_{1.7}$.

Fig. 4 shows the zero field cooling (ZFC) and field cooling (FC) magnetization curves of Mn_2 prepared by the hydrothermal method measured under different magnetic fields. A kink is observed at about 13 K in Fig. 4 (a) and (b), corresponding to the Néel magnetic transition temperature T_N . This temperature is lower than that of a MnO_2 single crystal [17] $T_N = 24.5$ K, which is due to the small grain size effect [19]. The kink as well as the difference between the ZFC and FC curves becomes smaller as the applied magnetic field increases. The inset in Fig. 4 (a) shows the ZFC and FC curves of the sample prepared at room temperature. A similar phenomenon is observed, except that the transition peaks are much broader and the magnetization value is higher which may be due to more defects and a larger distortion in this sample. Fig. 5 is the magnetization versus applied magnetic field curves of the sample prepared by the hydrothermal method. At 1.8 K, the M-H curve shows a small hysteresis, which indicates that a ferromagnetic component is superposed on the antiferromagnetic curve. This agrees with the M-T curves in that the magnetization increases with decreasing temperature suggesting a ferrimagnetic or ferromagnetic structure is formed in this compound. At 300 K, nearly linear M-H curves reveal that a paramagnetic

state exists in this temperature range. The ferromagnetic component at low temperature may result from the noncollinear molecular field that cants the two antiparallel sublattices due to the distortion of the crystal structure, especially arising from the oxygen vacancies. The small canted angle between the moments of the Mn sublattices leads to a small ferromagnetic moment [20].

I. SUMMARY

MnO₂ microspheres have been synthesized using hydrothermal and room temperature chemical reaction methods. The microspheres consist of MnO₂ nanowires having a diameter of 20–50 nm and a length of 2–8 μ m. The estimated value of the oxygen vacancy from XPS data is 0.3. The magnetic measurements indicate that MnO₂ has an antiferromagnetic structure with a parasitic ferromagnetic component below the Neel temperature, T_N . T_N is about 13 K which is 10 K lower than that of bulk MnO₂ single crystals.

II. ACKNOWLEDGMENTS

The support by DOE under DOE contract # DE-FC26-99FT400054 is acknowledged. We would like to thank A.G.S. Hemantha and Prof. J. Sweitz for help with the magnetic measurements.

REFERENCES

- [1] X.F. Daun, Y. Huang, Y. Cui, J.F. Wang, and C.M. Lieber, *Nature*(London) 409, 66 (2001).
- [2] J. Hu, M. Ouyang, P. Yang, and C.M. Lieber, *Nature*(London) 399, 48 (1999).
- [3] J.R. Heath, P.J. Kuekes, G. Snyder, and R.S. Williams, *Science* 280, 717 (1998).
- [4] M. Huang, S. Mao, H. Feick, H. Yan, Y. Wu, H. Kind, E. Weber, R. Russo, and P. Yang, *Science* 292, 1897 (2001).
- [5] A.R. Armstrong and P.G. Bruce, *Nature*(London) 381, 499 (1996).
- [6] B. Ammundsen and J. Paulsen, *J. Adv. Mater.*, 13, 943 (2001).
- [7] L.I. Hill, A. Verbaere, and D. Guyomard, *J. Power Sources* 119, 226 (2003).
- [8] Q. Li, J.B. Olson, and R.M. Penner, *Chem. Mater.*(2004) (in press).
- [9] S. Bach, J.P. Pereira-Ramos, and N. Barber, *J. Solid State Chem.* 120, 70 (1995).
- [10] J.C. Hunter, *J. Solid State Chem.* 39, 142 (1981).
- [11] M.H. Rossouw, D.C. Liles and M.M. Thackeray, *Mater. Res. Bull.*, 27, 221 (1997).
- [12] C. Wu, Y. Xie, D. Wang, J. Yang, and T. Li, *J. Phys. Chem. B* 107, 13583 (2003).
- [13] X. Wang and Y.D. Li, *J. Am. Chem. Soc.* 124, 2880 (2002); *Chem. Commun.*, 764 (2002).
- [14] M. Zhuang and J.W. Halley, *Phys. Rev B* 64, 024413 (2001).
- [15] H. Kawamura, *J. Appl. Phys.* 63, 3086 (1988).
- [16] H. Sato, K. Wakiya, T. Enoki, T. Kiyama, Y. Wakabayashi, H. Nakao, Y. Murakami, *J. Phys. Soc. Japan*, 70, 37 (2001).
- [17] N. Yamamoto, T. Endo, M. Shinada, and T. Takada, *Jap. J. Appl. Phys.* 13, 723 (1974).

- [18] Handbook of X-ray Photoelectron Spectroscopy, Edited by J. Chastain, Perkin-Elmer Corporation, Physical Electronic Division, USA. pp79.
- [19] Kh.Ya.Mulyukov, R.Z.Valiev, G.F.Korznikova, V.V.Stolyarov, Phys. Stat. Sol. (a), 112, 137 (1989).
- [20] V.E.Naish and E.A.Turov, Fiz.Met.Metalloved. 11, 321 (1961); 9, 10 (1960).

FIGURES

FIG .1. X-ray diffraction patterns of the sample prepared by the hydrothermal method (a) and room temperature reaction (b).

FIG .2. The SEM (a-d) and TEM (e) images of the Mn-oxides: (a), (b) prepared by hydrothermal method; (c) and (d) prepared at room temperature; (e) TEM image prepared by hydrothermal method.

FIG .3. Room temperature x-ray photoelectron spectrum of MnO_2 prepared by the hydrothermal method.

FIG .4. The temperature dependence of the magnetization curves under zero field cooling (ZFC) and field cooling (FC) for MnO_2 prepared by the hydrothermal method: (a) $H = 50 \text{ Oe}$, (b) $H = 1 \text{ kOe}$, (c) $H = 10 \text{ kOe}$. The inset in Fig. 4 (a) is for the sample made at room temperature.

FIG .5. The magnetization versus applied magnetic field curves of MnO_2 prepared by the hydrothermal method at different temperatures.

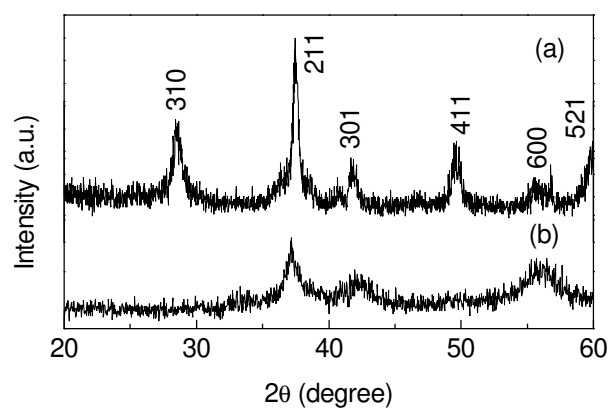


Fig. 1 Yang et al.,

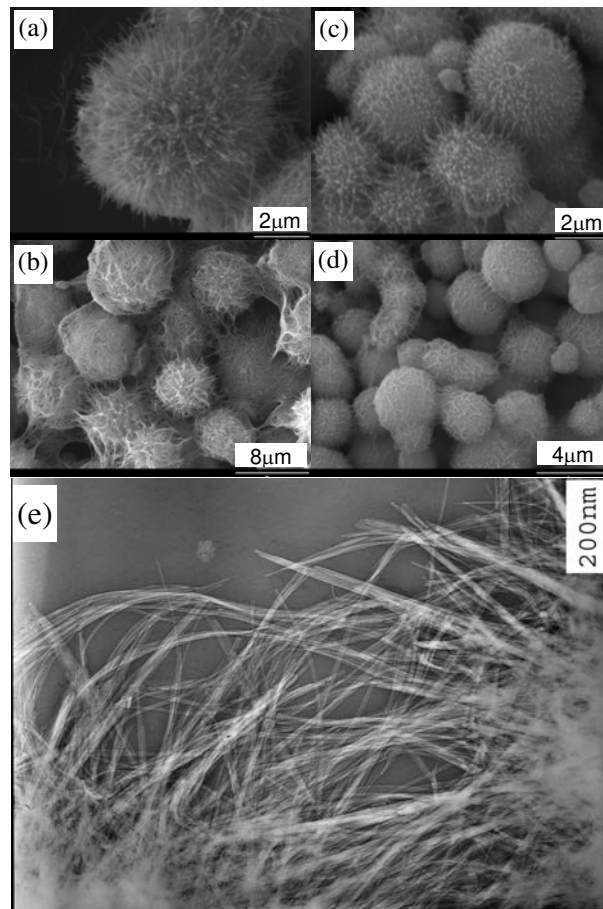
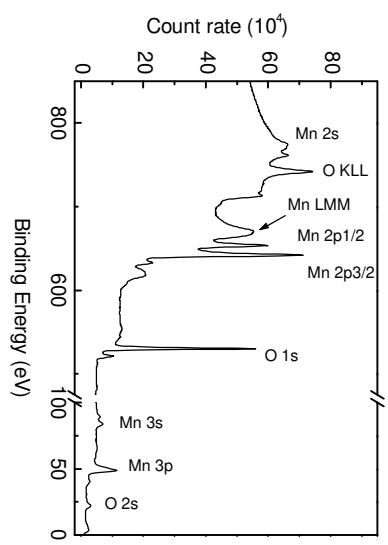


Fig. 2 Yang et al.,



Yang et al., Fig. 3

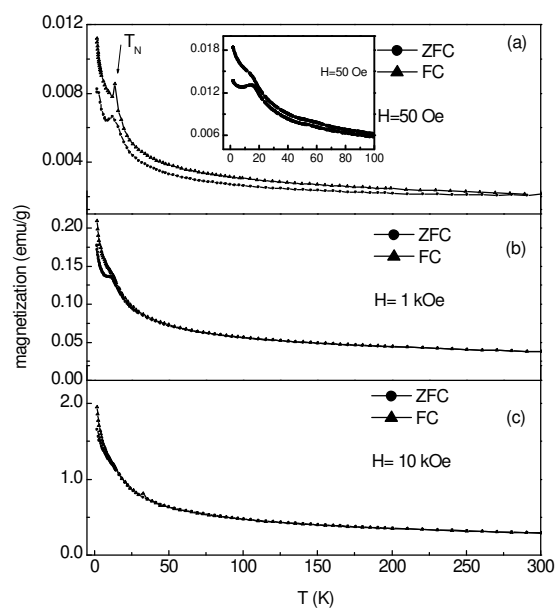
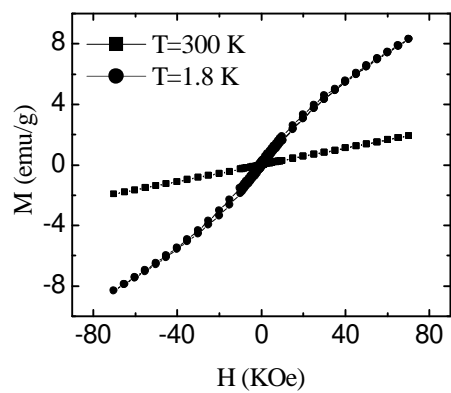


Fig. 4 Yang et al.,



Yang et al., Fig. 5

